COLLECTIVE ACCELERATION OF LASER PRODUCED IONS*

J. T. Cremer and W. W. Destler

Electrical Engineering Department
University of Maryland
College Park, Maryland 20742

Summary

Experimental studies of the collective acceleration of laser produced ions have been conducted. An intense relativistic electron beam (1 MeV, 30 kA, 30 ns) is emitted from a 4 mm diameter tungsten cathode and passes through a 2.4 cm hole in a stainless steel anode into a 14 cm diameter downstream drift tube. Ions are provided on the downstream side of the anode plane by firing a 4-10 J, 15 ns Q-switched ruby laser pulse at solid or foil targets mounted on the downstream side of the anode plane. Accelerated ion energies are measured using time of flight and range energy/track etching techniques. Ion charge states are measured using an E‖B Thomson spectrometer. Results will be compared with measurements of the pre-acceleration characteristics of the laser produced ions from these target geometries obtained using an electrostatic analyzer.

Introduction

Studies of the collective acceleration of ions from an independently controllable ion source using an intense linear electrom beam have been conducted in our laboratory at the University of Maryland for the past several years.[1-6] This work was a natural outgrowth of early experiments by Graybill, et al[7] and Luce[8] who initially investigated collective acceleration in the gas-filled and evacuated drift tube geometries, respectively. This early work was followed by experimental and theoretical investigation of this phenomena at several other laboratories,[9-13] as well as our own. During this period, we have reported the acceleration of a large number of ion species from puff-valve and laser-target ion sources to peak energies of about 5 MeV/amu independent of the ion mass. In these experiments, the electron beam pulse was 1-1.5 MeV, 30 kA, 30 ns FWHM. Protons have been accelerated to energies of 16-20 MeV in related experiments.

Initial experiments[4] of the collective acceleration of laser produced ions reported by our group indicated that although laser preionization did not result in higher peak ion energies, it did appear to increase the number of ions that are accelerated to high energy (3-5 MeV/amu). For this reason, we have initiated a systematic study of this configuration in which the characteristics of the laser-produced plasma from different target configurations have been measured using an electrostatic analyzer. The ion energies and charge states of the preaccleration plasma can then be compared to those measured after collective acceleration occurs.

Studies of Laser Produced Plasmas from Solid and Foil Metallic Targets

A comparative study of laser produced ions from solid and foil metallic targets has been performed in which an electrostatic analyzer and biased charge collectors were used as diagnostics. The experimental configuration is shown in Fig. 1. A Q-switched, 4-10 J, 15 ns ruby laser is focused to 10^{11} W/cm^2 on solid Al, Fe, and Ta targets and on .0003" Al foil, .0004" Fe foil, and .0002" Ta foil targets for various angle pairs (θ_i, θ_d), where θ_i is the angle of laser incidence and θ_d is the angle of ion detection. Data has been obtained for angle pairs with respect to the target normal of (5°,0°), (40°,45°), (0°,45°), (45°,0°), (22.5°,22.5°) and (180°,0°). The relative ion charge state distribution is measured using a 127° electrostatic analyzer located about 2 m from the target. In the analyzer detector, ions produce secondary electrons when they strike an aluminum knob biased to -20 kV, and the secondary electrons are accelerated onto NE102 scintillant, where the light produced is detected using a photomultiplier tube. A typical result of these studies is shown in Fig. 2, where the relative ion number for each charge state is plotted as a function of ion energy. It is easily seen that for the solid aluminum target results shown, the ion population is predominantly in charge states 1-3, with a maximum charge state observed of 5. An indication of the actual ion current has been obtained using biased charge collectors located 20 cm from the target. The current collected, if assumed to be in the same charge state distribution as that measured by the electrostatic analyzer, can be used to obtain a rough estimate of the total ion number. For this particular case, it is estimated that about 10^{16} Al ions are produced from the target on each shot.

It is interesting to compare this number with the total number of atoms vaporized by the laser as obtained from measurements of the volume of the pit in the solid produced by the laser. For this case, such measurements show that about 10^{19} atoms are liberated from the surface of the solid, an indication that only a small fraction of these atoms are ionized.

The complete results of this survey are too extensive to be detailed here. The main conclusions of the study are as follows: 1) The highest charge states and ion currents are observed when $\theta_i = 0°$ and $0° \leq \theta_i \leq 45°$ for all targets, 2) Solid targets deliver substantially more ion current at all charge states than do thin foil targets, and 3) The highest charge states observed are Z = 6 for aluminum and Z = 5 for iron and tantalum.

Collective Acceleration of Laser Produced Ions

The general experimental configuration used for these studies is shown in Fig. 3. An intense relativistic electron beam (1 MeV, 30 kA, 30 ns FWHM) is emitted from a 4 mm diameter cold tungsten cathode. The anode, a 6 mm thick stainless steel plate, has a 24 mm diameter hole on axis through which the beam passes into the downstream drift region. The diameter of the downstream drift tube is 14 cm. Ions to be accelerated are provided by firing a 4-10 J, 15 ns Q-switched ruby laser at solid or foil targets mounted in the downstream drift region. The timing of the laser firing must be adjusted such that ions are produced before electron beam injection, but not so early as to short the diode. In these experiments, a laser-electron beam firing delay of 0.5 microseconds was found to be optimum. Accelerated ions are usually not observed when the laser is not fired.

* Work supported by the Air Force Office of Scientific Research and the U.S. Department of Energy

0018-9499/83/0800-3186$01.00©1983 IEEE

Effect of Target Geometry.

A variety of different target geometries were tested, including 1) Foil targets stretched across the anode hole and irradiated on axis by the laser just before electron beam injection, 3) Wire targets (1 mil diameter) stretched across the anode hole in a similar fashion, 3) Rods (62 mil diameter) installed in a manner similar to the wire, and 4) Solid targets mounted off axis on the downstream side of the anode plane, as shown in Fig. 3. A typical ion time of flight measurement is shown in Fig. 4. In this case, the ion time of flight between two charge collection probes 30 cm apart is measured after any accompanying electrons are swept away using a transverse magnetic field. The photograph shown is for an off-axis aluminum solid target, and indicates a peak velocity of about 0.1 c, or about 5 MeV/amu. The peak ion energies obtained in this manner for the various target geometries are shown in Fig. 5. It is interesting to note that all of the configurations that potentially perturb the electron flow through the anode hole (wire, rod, and foil targets) resulted in lower peak accelerated ion energies than did the off-axis targets. All subsequent measurements have been performed with off-axis targets.

Charge State Measurements

Accelerated ion charge states were measured using a Thomson E||B spectrometer (see Fig. 3) similar to that designed by M. J. Rhee.[14] The ion beam is first collimated by two 0.3 mm pinholes separated by 23 cm. A magnetic field transverse to the collimated beam is provided by a permanent magnet and two pole pieces located inside the drift chamber. An insulated conducting plate located on the inside surface of one pole piece is connected to a high voltage power supply to provide an electric field parallel to the magnetic field. Typical values for E and B are 6 x 10^5 V/m and 0.15 T, respectively. Ions deflected by these fields are detected by a CR-39 track plate located 2.1 cm downstream of the pole pieces. The ion tracks become visible under a microscope after the exposed plate is etched in an NaOH solution.

Ions of a given charge to mass ratio Z/A and varying energy trace out a parabola on the track plate given theoretically by

$$x = \frac{5.2 \times 10^{-9} E_x [(L_1^E)^2 + 2L_1^E L_2^E)] y^2}{\frac{Z}{A}\left[\int_0^{L_1^B} \int_0^z B_x(z)\,dz\,dz\right]^2} \text{ (meters)}$$

where x is the coordinate in the direction of E and B (and therefore the direction of electric field deflection) and y is the direction of magnetic field deflection. The distance L_1^E over which the electric field is applied is assumed to be equal to the pole piece axial length. The post electric field drift distance to the track plate is L_2^E, and L_1^B is the distance over which the magnetic field is applied (in this case $L_2^B = 0$).

Fig. 6 is a photograph of a typical track plate. The coordinate axes and origin are obtained by setting either E_x or B_x to zero, or both, and accelerating ions in the normal fashion. The results of these measurements are summarized in Table I. It is easily seen that the highest charge state observed increases with ion mass. Peak energies determined from these measurements were in the range 1-2 MeV/amu, although Thomson spectrometry is not a particularly good diagnostic for determining ion energy, since resolution is poorest at high energy. This lower peak ion energy is attributable to the fact that the beam energy was about 1 MeV in this case, as compared to about 1.5 MeV in the time of flight measurements of ion energy.

In contrast to previous studies of the collective acceleration of ions from a localized gas cloud,[3-6] impurity contamination (particularly by protons) of the accelerated ion beam is a common occurrence. This contamination can be reduced, but not eliminated, by firing the laser at the target to clean the surface immediately before a shot. The results for tantalum and iron are diffcult to interpret, because the resolution of the spectrometer is not good enough to resolve individual charge states. In addition, tantalum has a high adsorption coefficient, and proton (and possibly nitrogen) contamination of the ion beam is routinely observed. When accelerated protons are observed, however, they are accelerated to approximately the same peak velocity as the fastest heavy ions. In the previous studies of the collective acceleration of ions from a localized gas cloud, it was also observed that all charge states were accelerated to approximately the same peak velocity.[6] Within experimental error, this appears to be the case in this work as well. These results appear to imply that the acceleration process is not electrostatic, in which case higher charge state ions should reach higher energies, but more likely the result of a moving potential well acceleration process similar to that used by Olson to describe ion acceleration in the gas filled geometry.[9]

Range-energy measurements of the accelerated ion energy are consistent with those obtained from the ion time of flight measurements, except when protons are present as contaminants in significant numbers (e.g. for Ta). This is a result of the fact that in this energy regime, the proton range is much greater than the heavy ion range for the same energy/nucleon.

References

1. W. W. Destler, L. Floyd, and M. Reiser, IEEE Trans. Nucl. Sci. 26, 4177 (1979).
2. W. W. Destler, L. E. Floyd, and M. Reiser, Phys. Rev. Lett. 44, 70 (1980).
3. L. E. Floyd, W. W. Destler, M. Reiser, and H. M. Shin, J. Appl. Phys. 52, 693 (1981).
4. W. W. Destler, L. E. Floyd, J. T. Cremer, C. R. Parsons, M. Reiser, and J. W. Rudman, IEEE Trans. Nucl. Sci. 28, 3404 (1981).
5. W. W. Destler and J. T. Cremer, J. Appl. Phys. 54, 636 (1983).
6. W. W. Destler, Rev. Sci. Inst. 54, 253 (1983).
7. S. Graybill and J. Uglum, J. Appl. Phys. 41, 236 (1970).
8. J. S. Luce, Ann. N. Y. Acad. Sci. 20, 336 (1973).
9. C. L. Olson and U. Schumacher, in Springer Tracts in Modern Physics: Collective Ion Acceleration, edited by G. Hohler (Springer, New York, 1979), Vol. 84.
10. J. A. Nation, G. Providakes, and V. Serlin, in Proceedings of the Fourth International Topical Conference on High Power Electron and Ion Beam Reserach and Technology, Palaiseau, France, 1981, p. 667.
11. L. S. Bogdankevich I. L. Zhelyazkov, and A. A. Rukhadze, Sov. Phys, JETP 30, 174 (1970).
12. M. Masuzaki, Y. Tamagawa, K. Kamada, S. Watanabe, S. Kawasaki, Y. Kubota, and T. Nakanishi, Jpn. J. Appl. Phys. 21, L326 (1982).
13. J. W. Poukey and N. Rostoker, Plasma Phys. 13, 897 (1971).
14. M. J. Rhee, IEEE Trans. Nucl. Sci. 28, 2663 (1981).

TABLE I. Results of charge state measurements.

Target Material	Z_{max}/A	$W_{max}(\frac{MeV}{amu})$	Observed Impurities
Carbon	5/12	~ 2	H^+
Aluminum	10/27	~ 1	H^+
Iron	~ 15/56	~ 1.5	H^+, H_2^+
Tantalum	~ 45/181	~ 1	H^+

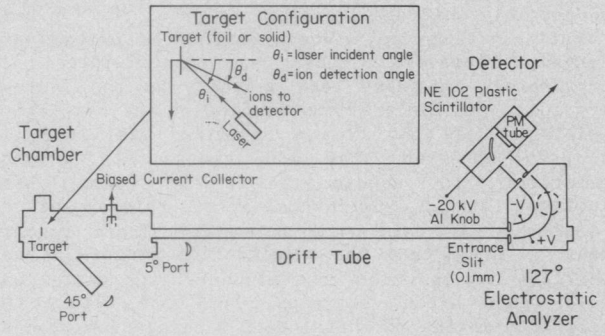

FIG. 1 Experimental configuration for studies of laser produced ions from solid and foil metallic targets.

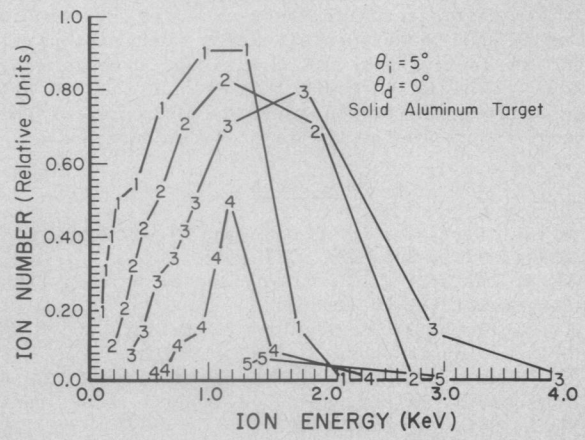

FIG. 2 Typical ion energy spectra for Al^{+1} to Al^{+5} as observed with the electrostatic analyzer.

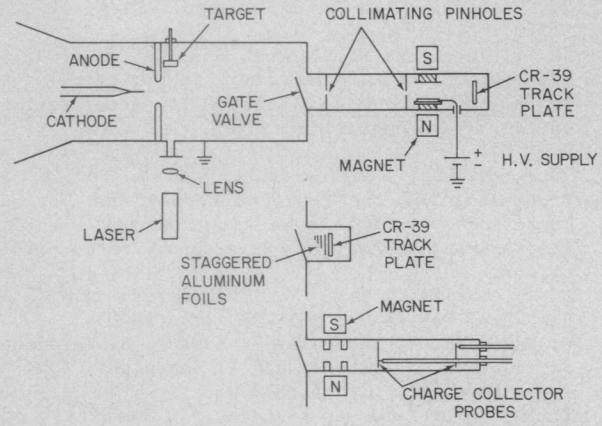

FIG. 3. Experimental configuration for studies of the collective acceleration of laser produced ions.

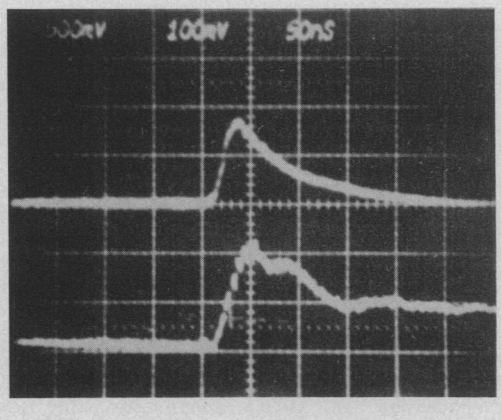

FIG. 4. Typical ion current waveforms from ion time of flight studies. Top trace--front probe, 3 A/division, bottom trace--back probe (30 cm downstream), 0.1 A/division.

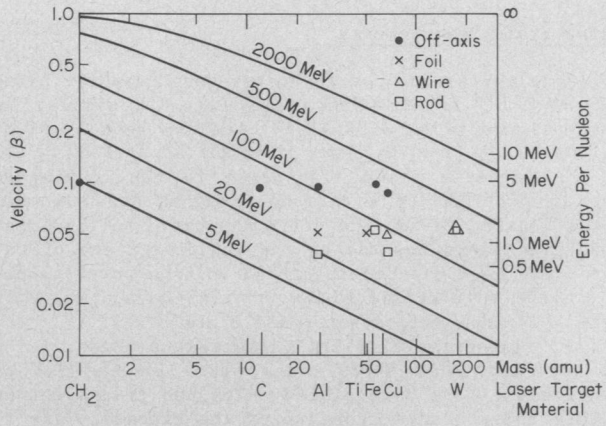

FIG. 5. Peak ion velocity for various target geometries and materials.

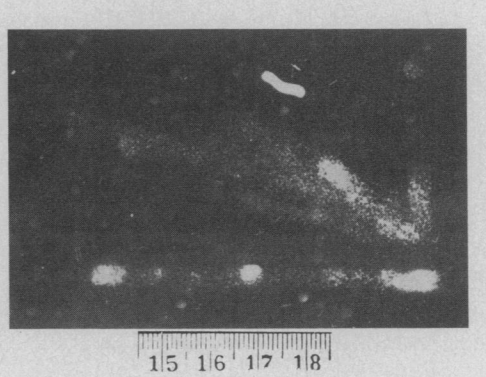

FIG. 6 Microscope photograph of typical Thomson spectrometer track plate for carbon ions. Each small division corresponds to 0.1 mm.